Zinc-Doped Titania Embedded on the Surface of Zirconia: A Potential Visible-Responsive Photocatalyst Material

Azizia Alifi, Rian Kurniawan, and Akhmad Syoufian*

Department of chemistry, Faculty of Mathematics and Natural Sciences, Universitas Gadjah Mada, Sekip Utara, Yogyakarta 55281, Indonesia

** Corresponding author:*

email: akhmadsyoufian@ugm.ac.id

Received: November 5, 2019
Accepted: February 4, 2020

DOI: 10.22146/ijc.51172

Abstract: *The preparation and characterization of zirconia-supported titania with a zinc dopant had been studied. Zinc-doped titania was grown on the surface of zirconia by the sol-gel method. Various zinc contents and calcination temperatures were applied to investigate the zinc doping effect and crystal structure of the zirconia-titania composite. X-ray diffraction method, Fourier-transform infrared spectroscopy, and UV-Vis reflectance spectroscopy were performed to characterize the composite. The morphology of the composite was observed by using a scanning electron microscope, and its composition was analyzed by using energy dispersive spectroscopy. Among various zinc dopant contents and calcination temperatures investigated, doping with 5% zinc (Zn wt./Ti wt.) at 900 °C calcination shows the best result in response to visible light with a bandgap of 2.87 eV and absorption edge wavelength of 432.61 nm.*

Keywords: *titania; zinc; zirconia; sol-gel; doping*

■ INTRODUCTION

TiO_2 has a high photoactivity under ultraviolet light irradiation because of its large bandgap (3.25 eV for anatase). However, solar light consists of 5% UV light (300–400 nm) and 43% visible light (400–700 nm). That is, the UV light only occupies a small portion of the sunlight, and a large part of solar energy cannot be utilized. TiO_2 also shows a higher recombination rate of photogenerated electrons and holes [1]. The photocatalytic performance of TiO_2 can be effectively improved through transition metal doping. Among other metals, Zn has drawn considerable attention because of its superior doping effect on the improvement of TiO_2 photocatalytic performance under visible irradiation [2-3]. Seabra et al. reported that the inhibition of anatase-to-rutile transformation and the increment of specific surface area are responsible for the improvement of TiO_2 photocatalytic performance under visible irradiation by zinc doping [2].

Titania has also been combined with other semiconductors such as zirconium dioxide (ZrO_2). ZrO_2 is a versatile material due to its properties, such as high chemical inertness, photochemical stability, good wear resistance, and a wide bandgap [4]. ZrO_2 has been used in several studies to increase the photocatalytic activity of TiO_2 because the coupling of the two semiconductors can achieve a more efficient charge separation, prolong the lifetime of charge carriers, and significantly minimize the recombination probability between the hole and electron [5-6]. The reported value of ZrO_2 bandgap energy (E_g) is in the range of 3.25 to 5.1 eV, limiting the spectrum of photons that can create electron-hole pairs to participate in oxidation or reduction reactions under the UV light [7-8].

A hybrid of TiO_2 and ZrO_2 has advantageous properties, such as high mechanical strength, high surface area, non-toxicity, corrosion resistance, and photocatalytic activity under sunlight [9]. The combination of TiO_2 and ZrO_2 inhibits the electron-hole recombination process, which enhances the lifetime of charged carriers, thus improving the photocatalytic activity [10]. Fan et al. conducted a photocatalytic degradation of rhodamine B using the TiO_2-ZrO_2 binary system under visible light irradiation. Results showed a promising photocatalytic activity under the visible-light region [11]. The bandgap of titania-zirconia composite

was found to be increasing with a decrease in crystallite and particle size [12-13]. The presence of ZrO_2 in TiO_2 inhibits the anatase-to-rutile phase transformation [14].

Herein, a series of zinc-doped titania was embedded on the zirconia surface by the sol-gel method. Titania was grown on the surface of zirconia to form a composite with higher thermal stability compared to pristine TiO_2. Zinc dopant was incorporated into the TiO_2 structure in order to shift the absorption ability of the composite to the visible range. Sol-gel route was preferred due to its low cost, easy compositional control, and low processing temperature [15]. Various zinc contents (from 1 to 9%) and calcination temperatures (from 500 to 900 °C) were applied to zirconia supported titania to evaluate the absorption shift and crystal structures.

■ EXPERIMENTAL SECTION

Materials

Titanium(IV) tetraisopropoxide (TTIP) (97%, Sigma Aldrich), and zirconia powder (ZrO_2) (Jiaozuo Huasu) were chosen as titania (TiO_2) precursor and supporting material, respectively. Zinc chloride ($ZnCl_2$) (Merck) was used as a dopant source. Absolute ethanol (PA, Merck) and demineralized water (Jaya Sentosa) were used as solvents.

Instrumentation

X-ray powder diffractometer (XRD) PANalytical X'Pert PRO MRD (Cu Kα radiation λ = 1.54 Å, 40 kV, 30 mA) was used to analyze the crystalline structure of composites. Vibrational spectra were measured on a Fourier transform infrared spectrophotometer (FT-IR, Thermo Nicolet Is10). Specular reflectance UV-Vis spectrometer UV 1700 Pharmaspec (SR-UV) was used to analyze the absorption of composites**.** Scanning Electron Microscope-Energy Dispersive X-Ray Spectrometer (SEM-EDX) FLEXSEM1000 with an accelerating voltage of 10 kV was used to analyze the morphology and elemental composition of synthesized composites.

Procedure

First, 2.5 mL of TTIP was diluted into 25 mL of absolute ethanol under mild stirring. Various amounts of $ZnCl_2$ and 1 g of ZrO_2 were mixed in 25 mL of demineralized water. The percentage of zinc dopant was fixed at 1, 3, 5, 7, and 9% to the weight ratio of titanium. The aqueous suspension was then added dropwise into the TTIP solution while being stirred. The mixture was stirred for another 30 min to maximize the reaction. Subsequently, the suspended solid was separated by centrifugation at 2000 rpm for 1 h. The obtained solid was aged in the open air for 24 h followed by the drying process in the oven at 80 °C for another 24 h. Ultimately, the dried solid was calcined under the atmospheric condition at 500 °C for 4 h with a ramp temp of 5 °C/min. Additionally, the composite with 5% zinc content was calcined further at 700 and 900 °C.

■ RESULTS AND DISCUSSION

The UV-Vis absorption spectra of Zn-doped TiO_2 embedded on the surface of ZrO_2 together with pure TiO_2 as a reference are shown in Fig. 1, and the corresponding calculated bandgaps are summarized in Table 1. The UV-Vis absorption of the composite was measured to demonstrate the doping effect of Zn in the TiO_2 structure. The bandgap energy (E_g) value for TiO_2 is 3.12 eV, while Zn-doped TiO_2 on ZrO_2 composites range from 3.08 to 2.87 eV. The increment of Zn content shifted the bandgap energy toward a longer wavelength. The bandgap decreased with the increasing of Zn content until the optimum condition of 5%, which exhibits the lowest bandgap of 2.87 eV. Zinc metal doping

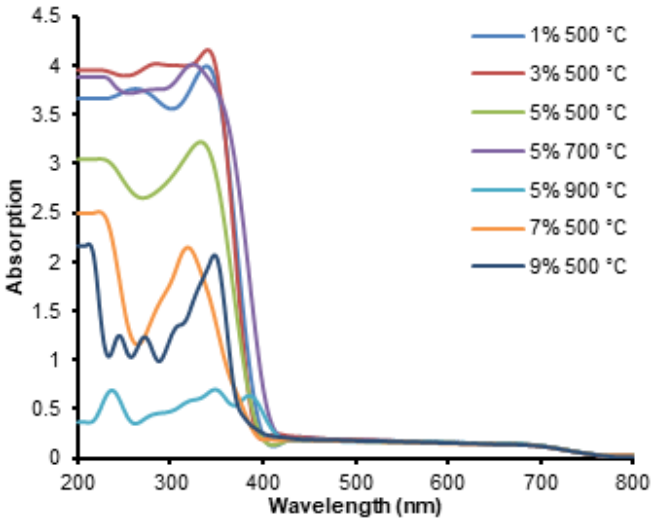

Fig 1. UV-Vis absorption spectra of various Zn-doped TiO_2 on ZrO_2 composites

Table 1. Bandgap data of pure TiO_2 and composites of Zn-doped TiO_2 on ZrO_2

Sample	E_g (eV)
TiO_2 500 °C	3.12
Zn-doped TiO_2-ZrO_2 1% 500 °C	3.07
Zn-doped TiO_2-ZrO_2 3% 500 °C	2.99
Zn-doped TiO_2-ZrO_2 5% 500 °C	2.90
Zn-doped TiO_2-ZrO_2 5% 700 °C	2.89
Zn-doped TiO_2-ZrO_2 5% 900 °C	2.87
Zn-doped TiO_2-ZrO_2 7% 500 °C	2.98
Zn-doped TiO_2-ZrO_2 9% 500 °C	3.08

in TiO_2 structure introduces new energy levels into the bandgap of TiO_2. When zinc is doped into TiO_2 lattice, some of the newly occupied molecular orbitals located below the conduction band (CB) of TiO_2 are formed. Therefore, this redshift and enhanced light absorption are attributed to the charge transfer from the dopant energy level of Zn to the CB of TiO_2 or O 2p to Zn 3d instead of Ti 3d [16]. The absorption of TiO_2-ZrO_2 composite with 7% and 9% of zinc contents returned to the lower wavelength due to the aggregation of ZnO formed during calcination. The increasing calcination temperature from 500 to 900 °C decreased the bandgap energy. It was caused by the phase transformation of TiO_2 from anatase to rutile. The E_g of rutile phase (3.0 eV) is lower than that of the anatase crystal phase (3.2 eV). Thus, the bandgap energy of the sample calcined at 900 °C was lower than samples calcined at 500 and 700 °C.

Fig. 2 shows the surface morphology and corresponding EDX spectra of pure TiO_2 and 5% Zn-doped TiO_2 on the ZrO_2 composite calcined at 500 °C. The elemental composition of the samples obtained from EDX measurements is given in Table 2. The EDX images of elementals distribution of Zn-doped TiO_2 on the ZrO_2 composite calcined at 500 °C are shown in Fig. 3. It can be seen that the undoped TiO_2 particle morphology is spherical in general, and Zn-doped TiO_2 on the ZrO_2 composite looks rougher feature than TiO_2. It is clear from the elemental analysis that 0.95% of the Zn element was present in the doped samples. In addition,

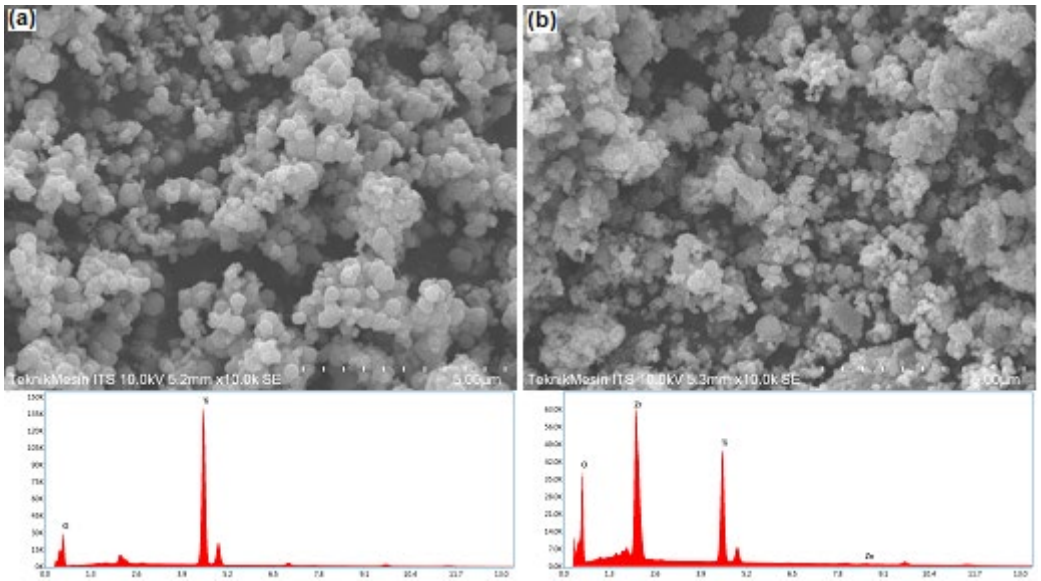

Fig 2. SEM images and EDX spectra of (a) TiO_2 and (b) 5% Zn-doped TiO_2 on ZrO_2 composite calcined at 500 °C

Table 2. Elemental surface composition of TiO_2 and 5% Zn-doped TiO_2 on ZrO_2 composite both calcined at 500 °C

Material	% Mass				
	Zr	O	Ti	Zn	Total
TiO_2	-	36.82	63.18	-	100
5% Zn-doped TiO_2-ZrO_2	31.16	41.51	26.39	0.95	100

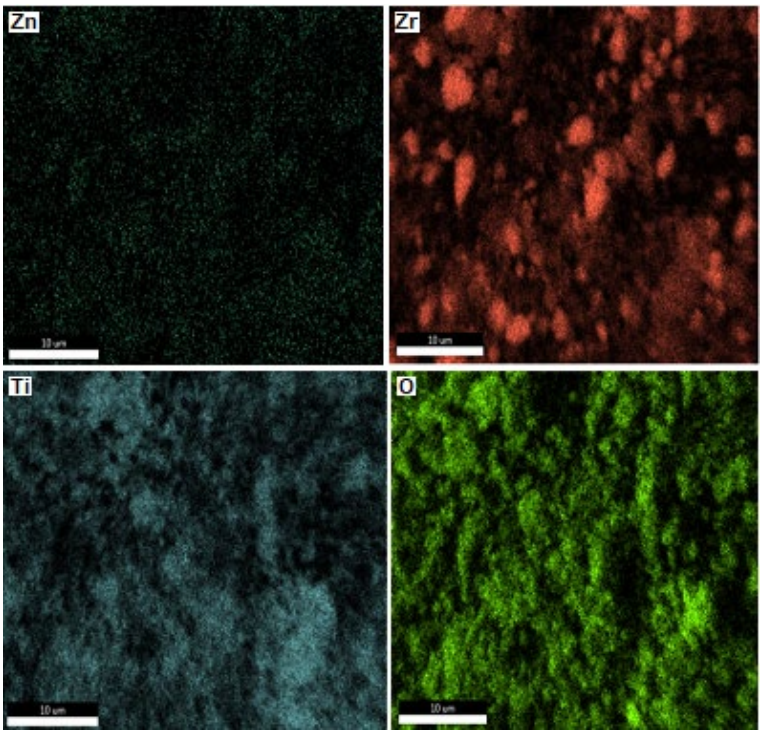

Fig 3. Elemental mapping images of 5% Zn-doped TiO_2 on ZrO_2 composite calcined at 500 °C

it can be revealed from the analysis that Zn had been successfully incorporated on the surface of the TiO_2-ZrO_2 composite. EDX spectra and data confirm that there was no impurity in the samples.

XRD patterns of undoped and Zn-doped TiO_2 on ZrO_2 composites together with pure TiO_2 calcined at 500 °C are shown in Fig. 4. Zn-doped composite calcined at 500 °C exists in two main crystalline forms, anatase and monoclinic, and no peak related to the rutile or any other phase is observed. Two main peaks of anatase TiO_2 are at 2θ of 25° (101) and 48° (200), which is closely matching with ICDD PDF number: 00-002-0387. On the other hand, XRD peaks of ZrO_2 at 2θ of 28° (-111), 31° (111), and 34° (020) are often taken as the characteristic peaks of monoclinic, which is closely matching with ICDD PDF number: 01-074-1200. The presence of the dopant was not found in the XRD patterns, which might be due to either the uniform distribution of dopant in TiO_2 lattice or the low amount of dopant used [17]. The presence of the Zn dopant in the composite was confirmed by EDX analysis, as discussed before. All composites exhibited lower-intensity peaks of anatase at 25° compared to pure TiO_2.

The XRD patterns of 5% Zn-doped TiO_2 on ZrO_2 composites calcined at different temperatures are presented in Fig. 5. XRD pattern of undoped TiO_2 calcined at 500 °C shows only anatase phase at 2θ of 25° (101) and 48° (200), while the XRD pattern of Zn-doped TiO_2-ZrO_2 composite displays a weak anatase peak at 2θ of 25° (101) and strong monoclinic peaks at 2θ of 28° (-111) and 31° (111). XRD pattern of Zn-doped TiO_2-ZrO_2 calcined at 700 °C had an emerging rutile peak at 2θ of 27° (110) and a diminished anatase peak at 25° (101). This suggests that there was a phase transformation from anatase to rutile at about 700 °C, which agrees with the previous experiment [18]. The diffraction peaks at 2θ = 27° (110), 36° (101), 41° (111), and 54° (211) correspond to the rutile phase (ICDD PDF number: 00-004-0551). After calcination at 900 °C, the anatase peak disappeared while the rutile peak became stronger than that at 700 °C. The presence of ZrO_2 and Zn dopant are presumably responsible for inhibiting the transformation of anatase to rutile [14,19-20].

FT-IR spectra of various Zn-doped composites together with pure TiO_2 are presented in Fig. 6. Absorption peaks around 500 and 545 cm^{-1} can be devoted to stretching vibration of the Ti–O bond and

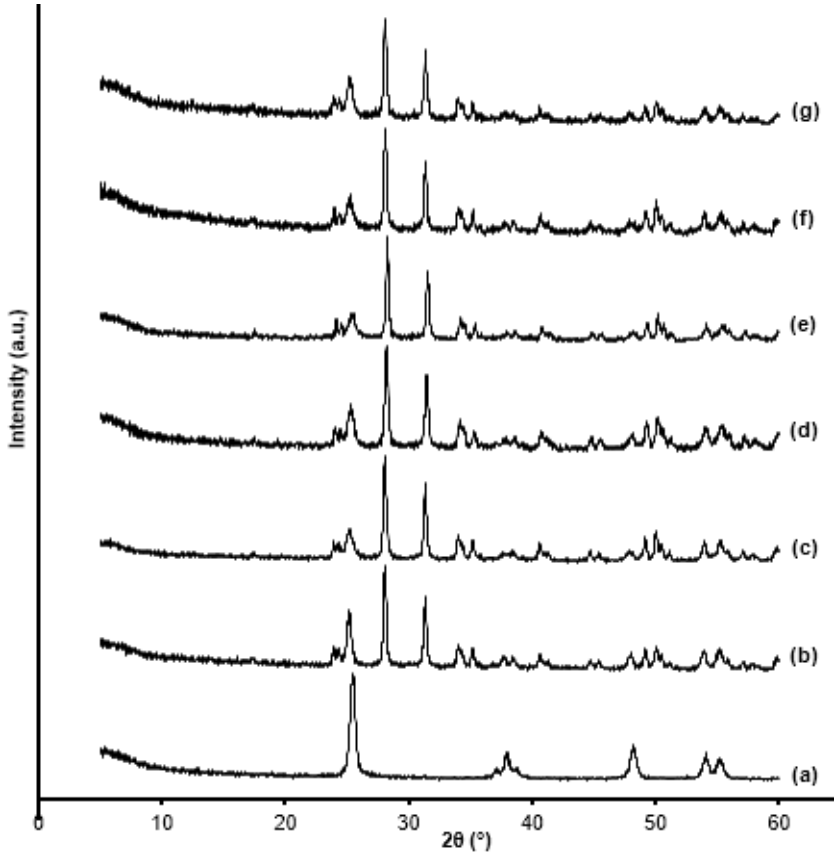

Fig 4. XRD patterns of (a) TiO_2, (b) undoped and Zn-doped TiO_2 on ZrO_2 composites with Zn content of (c) 1, (d) 3, (e) 5, (f) 7, (g) 9% (w/w) calcined at 500 °C

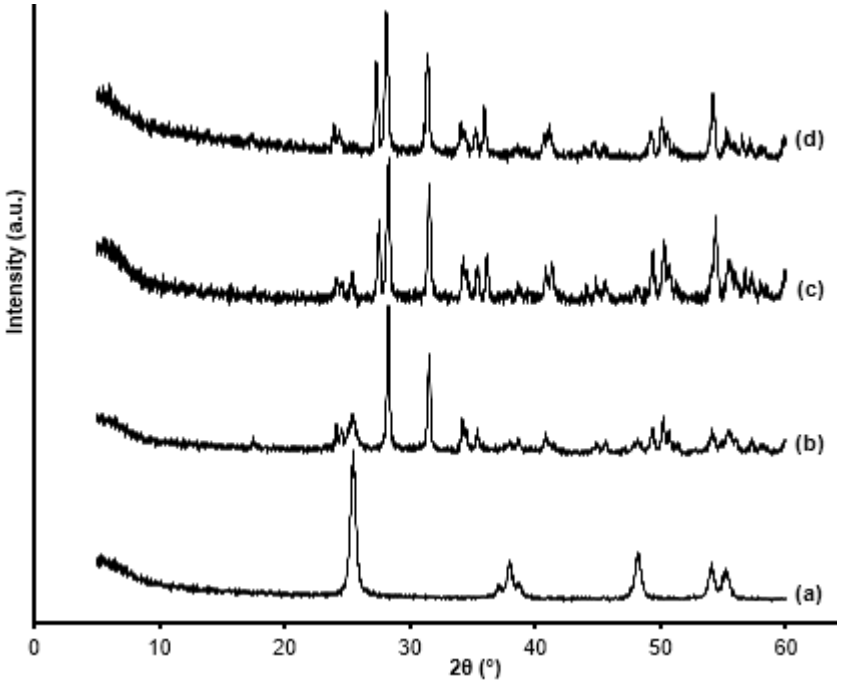

Fig 5. XRD patterns of (a) TiO_2 calcined at 500 °C, 5% Zn-doped TiO_2 on ZrO_2 composites calcined at (b) 500, (c) 700, and (d) 900 °C

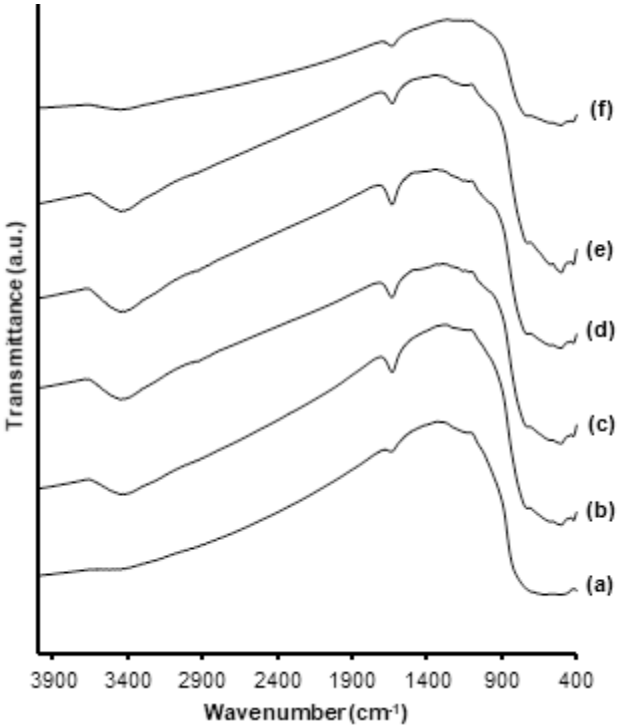

Fig 6. FTIR spectra of (a) TiO_2 and Zn-doped TiO_2 on ZrO_2 composites with Zn content of (b) 1, (c) 3, (d) 5, (e) 7, (f) 9% (w/w) calcined at 500 °C

Zr–O bond, respectively [21-22]. Peaks around 3100–3600 and 1632 cm^{-1} are assigned to stretching and bending vibrations of hydroxyl groups, respectively [23]. The absorption peaks of Ti–O and Zr–O tended to decrease as the Zn dopant content increased. It indicates that zinc metal was successfully doped into the TiO_2 structure. There was a new peak that appeared around 1200 $cm^{-1,}$ which may belong to Zn–O–Ti vibration at the substitutional position.

Fig. 7 shows the FTIR spectra of 5% Zn-doped TiO_2 on ZrO_2 composites calcined at different temperatures, together with TiO_2 calcined at 500 °C as a reference. After calcination at 700 °C, the O–H vibration bands became much weaker than those at 500 °C, indicating the removal of a certain amount of O–H groups during calcination. After heat treatment at a temperature of 900 °C, the spectra show further disappearance of O–H group peaks, indicating a complete elimination of hydroxy groups. The vibration band of Zn–O–Ti around 1200 cm^{-1} decreased when the calcination temperatures were increased. It was caused by dopant that sinters at high temperature [24].

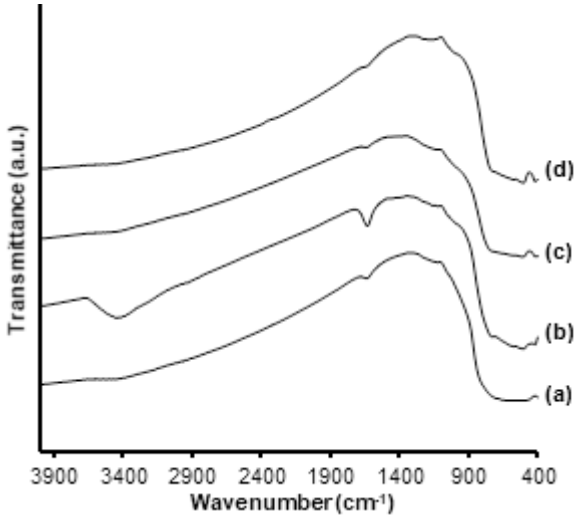

Fig 7. FTIR spectra of (a) TiO_2 calcined at 500 °C, 5% Zn-doped TiO_2 on ZrO_2 composites calcined at (b) 500, (c) 700, and (d) 900 °C

The visible-light-response of the synthesized composite based on UV-Vis spectral data gives an insight that the composite has potential as a photocatalyst. The zinc dopant shifts the absorption edge of TiO_2 to a higher wavelength, thus increasing the photocatalytic activity of TiO_2 hypothetically. Embedding TiO_2 on the surface of ZrO_2 was proven to inhibit the anatase-to-rutile transformation, thus establishing a relatively thermally stable composite compared to TiO_2.

■ CONCLUSION

A series of Zn-doped TiO_2 embedded on the surface of ZrO_2 with various zinc contents were successfully synthesized through the sol-gel method and calcined at different temperatures. Zn doping results in the improvement of photo-response under visible light irradiation. TiO_2-ZrO_2 composite with 5% of zinc content calcined at 900 °C exhibits the lowest bandgap of 2.87 eV with an absorption edge wavelength of 432.61 nm. The presence of ZrO_2 and Zn inhibits the anatase-to-rutile transformation at 700 and 900 °C of calcination temperatures. The experimental results demonstrate that doped TiO_2 embedded on the ZrO_2 surface with optimal Zn content can be considered as a promising photocatalyst under visible light irradiation.

■ ACKNOWLEDGMENTS

We would like to express our gratitude to the Faculty of Mathematics, and Natural Sciences Universitas Gadjah Mada for their support on this works through BPPTNBH 2019 Grant (86/J01.1.28/PL.06.02/2019).

■ REFERENCES

[1] Huang, F., Yan, A., and Zhao, H., 2016, "Influences of doping on photocatalytic properties of TiO_2 photocatalyst" in *Semiconductor Photocatalysis - Materials, Mechanisms and Applications*, Eds. Cao, W., IntechOpen, Rijeka, Croatia.

[2] Seabra, M.P., Salvado, I.M.M., and Labrincha, J.A., 2011, Pure and (zinc or iron) doped titania powders prepared by sol-gel and used as photocatalyst, *Ceram. Int.*, 37 (8), 3317–3322.

[3] Nair, R.G., Mazumdar, S., Modak, B., Bapat, R., Ayyub, P., and Bhattacharyya, K., 2017, The role of surface O-vacancies in the photocatalytic oxidation of methylene blue by Zn-doped TiO_2: A mechanistic approach, *J. Photochem. Photobiol., A*, 345, 36–53.

[4] Yao, N.Q., Liu, Z.C., Gu, G.R., and Wu, B.J., 2017, Structural, optical, and electrical properties of Cu-doped ZrO_2 films prepared by magnetron co-sputtering, *Chin. Phys. B*, 26 (10), 106801.

[5] Jiang, B., Zhang, S., Guo, X., Jin, B., and Tian, Y., 2009, Preparation and photocatalytic activity of CeO_2/TiO_2 interface composite film, *Appl. Surf. Sci.*, 255 (11), 5975–5978.

[6] Zheng, R., Meng, X., and Tang, F., 2009, Synthesis, characterization and photodegradation study of mixed-phase titania hollow submicrospheres with rough surface, *Appl. Surf. Sci.*, 255 (11), 5989–5994.

[7] Polisetti, S., Deshpande, P.A., and Madras, G., 2011, Photocatalytic activity of combustion synthesized ZrO_2 and ZrO_2–TiO_2 mixed oxides, *Ind. Eng. Chem. Res.*, 50 (23), 12915–12924.

[8] Králik, B., Chang, E.K., and Louie, S.G., 1998, Structural properties and quasiparticle band structure of zirconia, *Phys. Rev. B: Condens. Matter*, 57 (12), 7027–7036.

[9] Kubiak, A., Siwińska-Ciesielczyk, K., and Jesionowski, T., 2018, Titania-based hybrid materials with ZnO, ZrO_2 and MoS_2: A review, *Materials*, 11 (11), 2295.

[10] Zhang, J., Li, L., Zhang, J., Zhang, X., and Zhang, W., 2017, Controllable design of natural gully-like TiO_2-ZrO_2 composites and their photocatalytic degradation and hydrogen production by water splitting, *New J. Chem.*, 41 (17), 9113–9122.

[11] Fan, M., Hu, S., Ren, B., Wang, J., and Jing, X., 2013, Synthesis of nanocomposite TiO_2/ZrO_2 prepared by different templates and photocatalytic properties for the photodegradation of Rhodamine B, *Powder Technol.*, 235, 27–32.

[12] Gao, B., Lim, T.M., Subagio, D.P., and Lim, T.T., 2010, Zr-doped TiO_2 for enhanced photocatalytic degradation of bisphenol A, *Appl. Catal., A*, 375 (1), 107–115.

[13] Verma, S., Rani, S., Kumar, S., and Khan, M.A.M., 2018, Rietveld refinement, micro-structural, optical and thermal parameters of zirconium titanate composites, *Ceram. Int.*, 44 (2), 1653–1661.

[14] Andita, K.R., Kurniawan, R., and Syoufian, A., 2019, Synthesis and characterization of Cu-doped zirconium titanate as a potential visible-light responsive photocatalyst, *Indones. J. Chem.*, 19 (3), 761–766.

[15] Kong, L., Karatchevtseva, I., Holmes, R., Davis, J., Zhang, Y., and Triani, G., 2016, New synthesis route for lead zirconate titanate powder, *Ceram. Int.*, 42 (6), 6782–6790.

[16] Wang, Q., Yun, G., An, N., Shi, Y., Fan, J., Huang, H., and Su, B., 2015, The enhanced photocatalytic activity of Zn^{2+} doped TiO_2 for hydrogen generation under artificial sunlight irradiation prepared by sol-gel method, *J. Sol-Gel Sci. Technol.*, 73 (2), 341–349.

[17] Sikirman, A., Krishnan, J., and Mohamad, E.N., 2014, Effect of dopant concentration of N, Fe co-doped TiO_2 on photodegradation of methylene blue under ordinary visible light, *Appl. Mech. Mater.*, 661, 34–38.

[18] Kim, K.H., Park, H., Ahn, J.P., Lee, J.C., and Park, J.K., 2007, HRTEM study of phase transformation from anatase to rutile in nanocrystalline TiO_2 particles, *Mater. Sci. Forum*, 534-536, 65–68.

[19] Jing, L., Xin, B., Yuan, F., Xue, L., Wang, B., and Fu, H., 2006, Effects of surface oxygen vacancies on photophysical and photochemical processes of Zn-doped TiO_2 nanoparticles and their relationships, *J. Phys. Chem. B*, 110 (36), 17860–17865.

[20] Venkatachalam, N., Palanichamy, M., Arabindoo, B., and Murugesan, V., 2007, Enhanced photocatalytic degradation of 4-chlorophenol by Zr^{4+} doped nano TiO_2, *J. Mol. Catal. A: Chem.*, 266 (1-2), 158–165.

[21] Tsiourvas, D., Tsetsekou, A., Arkas, M., Diplas, S., and Mastrogianni, E., 2011, Covalent attachment of a bioactive hyperbranched polymeric layer to titanium surface for the biomimetic growth of calcium phosphates, *J. Mater. Sci. - Mater. Med.*, 22 (1), 85–96.

[22] Tamrakar, R.K., Tiwari, N., Dubey, V., and Upadhyay, K., 2015, Infrared spectroscopy and luminescence spectra of Yb^{3+} doped ZrO_2 nanophosphor, *J. Radiat. Res. Appl. Sci.*, 8 (3), 399–403.

[23] Gao, Y., Masuda, Y., Peng, Z., Yonezawa, T., and Koumoto, K., 2003, Room temperature deposition of a TiO_2 thin film from aqueous peroxotitanate solution, *J. Mater. Chem.*, 13 (3), 608–613.

[24] Kurniawan, R., Sudiono, S., Trisunaryanti, W., and Syoufian, A., 2019, Synthesis of iron-doped zirconium titanate as a potential visible-light responsive photocatalyst, *Indones. J. Chem.*, 19 (2), 454–460.